Dual-Wavelength-Modulation mm-Wave and THz Systems: Analysis and Experimental Demonstration At 60 GHz With a Gain-Switched Laser

Luis Gonzalez-Guerrero, Amol Delmade, *Member, IEEE*, Devika Dass, Colm Browning, *Senior Member, IEEE*, Liam Barry, *Senior Member, IEEE*, Frank Smyth, Horacio Lamela, and Guillermo Carpintero, *Senior Member, IEEE*

***Abstract*—Dual-wavelength-modulation (dual-λ-mod) photonic mm-wave/THz transmitters are an attractive alternative to conventional heterodyne systems for their simplicity. In this article, dual-λ-mod systems are analysed, paying special attention to the impact of fiber dispersion and signal-signal beat interference. In contrast to what has been reported in the literature, it is concluded here that dual-λ-mod systems based on optical double sideband (DSB) modulation are subjected to power fading, rendering them useless for high-speed mm-wave/THz communications. To solve this, the use of optical single sideband (SSB) modulation – which is immune to power fading – is proposed here. Using a gain-switched (GS) laser, a 60-GHz SSB dual-λ-mod system transmitting 2.5-GBd 16-QAM signals is demonstrated experimentally. A penalty of around 2.8 dB is measured with respect to the conventional dual-path heterodyne transmitter over optical B2B and 10-km transmission. The reduction in complexity enabled by the demonstrated system aids in the deployment of cost-effective mm-wave/THz networks.**

***Index Terms*—Mm-wave communications, THz communications, microwave photonics, radio-over-fiber.**

I. Introduction

MM-WAVE (30 GHz–300 GHz) and THz (100 GHz–1 THz) bands have atmospheric transmission windows (i.e., parts of the electromagnetic spectrum where the atmospheric attenuation is low) with bandwidths of several tens of GHz. These bands are considered a key resource to combat the spectrum congestion at lower radio frequencies (RFs). Hence, mm-wave/THz communications have become a very active research topic in the past few years [1], [2], [3], [4]. The highest transmission rates reported in these bands have been enabled by coherent photonic systems supporting complex modulation formats [5]. The conventional photonic approach to generate modulated mm-wave/THz carrier frequencies is based on the dual-path heterodyne system shown in Fig. 1(a). In this system, two correlated optical lines from a dual-λ generator are first demultiplexed, one of them is then modulated with the data, whereas the other one is left unmodulated to act as an optical local oscillator (LO). The modulated optical signal and the LO are then recombined and sent to the photodiode (PD), where they are mixed together producing the mm-wave/THz signal. This arrangement presents several problems [6]: first, as both lines travel through different optical paths, they can become

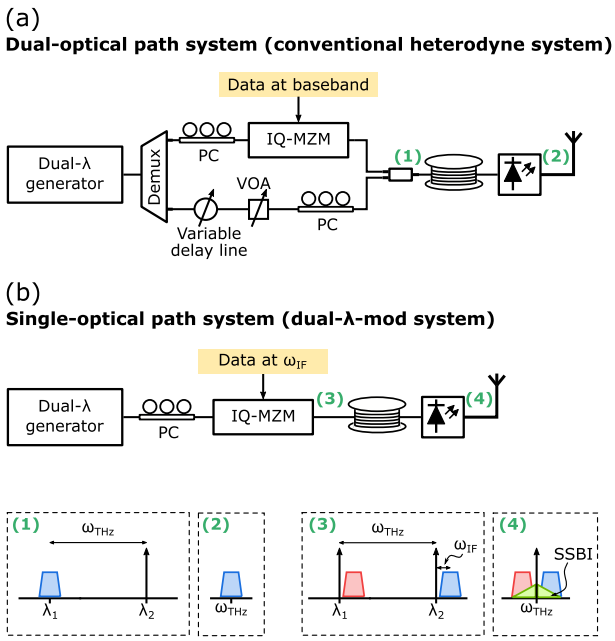

Fig. 1. Comparison between photonic transmitters for the generation of modulated mm-wave/THz carriers and their associated signal spectrum at different points. THz: mm-wave/THz frequency, VOA: variable optical attenuator, PC: polarization controller, IF: intermediate frequency, CW: continuous wave, SSBI: signal-signal beat interference. (a) Dual-optical path system (conventional heterodyne system). (b) Single-optical path system (dual-A-mod system).

Manuscript received 11 May 2023; revised 20 August 2023; accepted 6 September 2023. Date of publication 13 October 2023; date of current version 2 December 2023. This work was supported in part by UC3M and the European Commission under Grants GA 801538 and 101096949, in part by the Spanish Ministry of economic affairs and Digital Transformation under Grant TSI-063000-2021-136, and in part by Science Foundation Ireland under Grants 18/SIRG/5579, 13/RC/2077/p2, and 12/RC/2276/P2. *(Corresponding author: Luis Gonzalez-Guerrero.)*

Luis Gonzalez-Guerrero, Horacio Lamela, and Guillermo Carpintero are with Grupo de Optoelectronica y Tecnologia Laser (GOTL), 28911 Madrid, Spain (e-mail: lgguerre@ing.uc3m.es; horacio@ing.uc3m.es; guiller@ing.uc3m.es).

Amol Delmade, Devika Dass, Colm Browning, and Liam Barry are with the School of Electronic Engineering, Dublin City University, D09V209 Dublin, Ireland (e-mail: amol.delmade2@mail.dcu.ie; devika.dass2@mail.dcu.ie; colm.browning@dcu.ie; liam.barry@dcu.ie).

Frank Smyth is with Pilot Photonics Ltd., D09PH2K Dublin, Ireland (e-mail: frank.smyth@pilotphotonics.com).

Color versions of one or more figures in this article are available at https://doi.org/10.1109/JLT.2023.3322908.

Digital Object Identifier 10.1109/JLT.2023.3322908

decorrelated, increasing the phase noise of the generated mm-wave/THz signal. An optical delay line or more complex techniques [7] are required to mitigate this effect. Second, this arrangement needs an optical wavelength demultiplexer and a coupler to split and then recombine the two optical lines. Furthermore, the need to match both the polarization state and the power level of both signal arms makes the system rather complex.

All these problems can be solved by using a photonic transmitter with a single optical path as the one depicted in Fig. 1(b). In this system, the two optical tones from a dual-λ generator are modulated with the same data. Hence, this system is here referred to as a dual-λ-mod system. This system is similar to optical carrier-suppressed (OCS) systems but has two fundamental differences: first, in dual-λ-mod systems, phase data is suppressed upon photodetection (in OCS systems phase is doubled); second, the transmission frequency in dual-λ-mod systems is not limited by modulator bandwidth. This last feature, make dual-λ-mod systems more attractive for mm-wave/THz communications than OCS systems. The suppression of the phase data in dual-λ-mod systems represents a problem for the transmission of complex signals (i.e., signals with phase modulation). However, there are modulation techniques that allow to retrieve phase information in dual-λ-mod systems. One of the most popular such techniques consists on upconverting the complex signal into an intermediate frequency (IF) and then modulating it into the amplitude or intensity envelope of the optical signal [6].

Given their simplicity compared to conventional heterodyne systems (i.e., the system in Fig. 1(a)) and their easy scalability to high transmission frequencies, dual-λ-mod systems are a very interesting option for mm-wave/THz high-speed communications systems. In this article, dual-λ-mod systems are analysed in detail through both simulations and experimental transmissions. The structure of the paper is as follows:

- Section II discusses two impairments associated with dual-λ-mod systems: power fading due to optical dispersion and the signal-signal beat interference (SSBI).
- Section III presents possible wireless receiver arrangements for dual-λ-mod systems and reviews notable transmission experiments published in the literature.
- Section IV shows the experimental results obtained for a 60-GHz system based on a gain-switched (GS) laser together with its comparison with a conventional heterodyne system.
- Section V summarizes the main conclusions of the paper.

II. Transmission Considerations

A. Optical Dispersion

Most of the reported experiments on dual-λ-mod systems are based on double sideband with carrier (DSB-C) optical modulation. Hence, most of the studies on the effect of fiber dispersion in dual-λ-mod systems have focused on this type of modulation [8], [9], [10]. To easily understand the implications of dispersion on DSB-C dual-λ-mod systems, one can analyze the case where the modulating signal is a continuous wave (CW) signal. Fig. 2(a) shows the generated optical spectrum in this case for an angular CW frequency of ω_{IF}. As can be seen, there are four identical sidebands and two optical carriers. The phase shifts undergone by each of these spectral components due to the group velocity dispersion (GVD) of fiber are also shown in Fig. 2(a). If one now looks at the mm-wave/THz spectrum, it can be seen that the amplitude of the central carrier (the one with an angular frequency of ω_{THz} after photodetection) is fixed and does not depend on the GVD phase shifts. This is because this carrier is the product of a single beating and, hence, no interferometric effect occurs upon photodetection. According to this, it could be concluded that DSB-C dual-λ-mod systems do not suffer from power fading. This is the analysis presented in [8], where the authors state that DSB-C systems are immune to this undesired feature. This analysis, however, does not take into consideration the modulation sidebands.

If one now looks at the mm-wave/THz data sidebands (the ones with angular frequencies of $\omega_{THz} \pm \omega_{IF}$ after photodetection), it can be seen that each of them is the sum of two carrier-sideband beatings. This makes both sidebands have a dispersion-induced amplitude envelope ($\cos(\phi_3 - \phi_2)$ for the low-frequency sideband and $\cos(\phi_1 - \phi_2)$ for the high-frequency one) that depends on the GVD phase shifts φ_1, φ_1, and φ_3. These, in turn, depend on the transmission length l, the frequency separation between the two carriers ω_{THz}, and ω_{IF}. Taking the high frequency sideband as an example, since $\phi_1 = (-\beta_2/2)(\omega_{THz}/2 + \omega_{IF})^2\, l$ and $\phi_2 = (-\beta_2/2)(\omega_{THz}/2)^2\, l$ (where β_2 is the GVD of fiber), the dispersion-induced amplitude term $\cos(\phi_1 - \phi_2)$ is equal to $\cos((-\beta_2/2)(\omega_{IF}^2 + \omega_{IF}\,\omega_{THz})l)$. This is the same result given in 12 of [9]. On the other hand, as shown in Fig. 2(b), optical SSB formats prevent the occurrence of power fading in dual-λ-mod systems. This is because all components in the mm-wave/THz signal are the result of a single PD beating.

The effect of dispersion on dual-λ-mod systems can be seen in Fig. 3, which shows the mm-wave/THz spectrum obtained with simulations for (a) optical DSB-C modulation and (b) optical SSB-C modulation (the parameters used in the simulations are detailed in the caption of the figure). As expected, the mm-wave/THz sidebands obtained with optical DSB-C modulation exhibit the dips associated with power fading. As these sidebands convey all the information and are the only PD output that matters for communication, the authors of this manuscript believe it is more accurate to regard dual-λ-mod DSB-C systems as systems with power fading. The only difference between the system analyzed in [8] and the ones discussed here is that, in [8], real baseband modulation is assumed (i.e., $\omega_{IF} = 0$). Such signals will also exhibit the dips associated with power fading, however, as discussed at the beginning of this section, these dips will never occur at the central carrier of the generated mm-wave/THz signal (since it is the product of a single PD beating). Of course, for baseband or low-ω_{IF} narrow-bandwidth DSB-C signals, only very long distances of fiber will lead to power dips. However, given the high transmission speeds envisaged for mm-wave/THz communications, power fading is

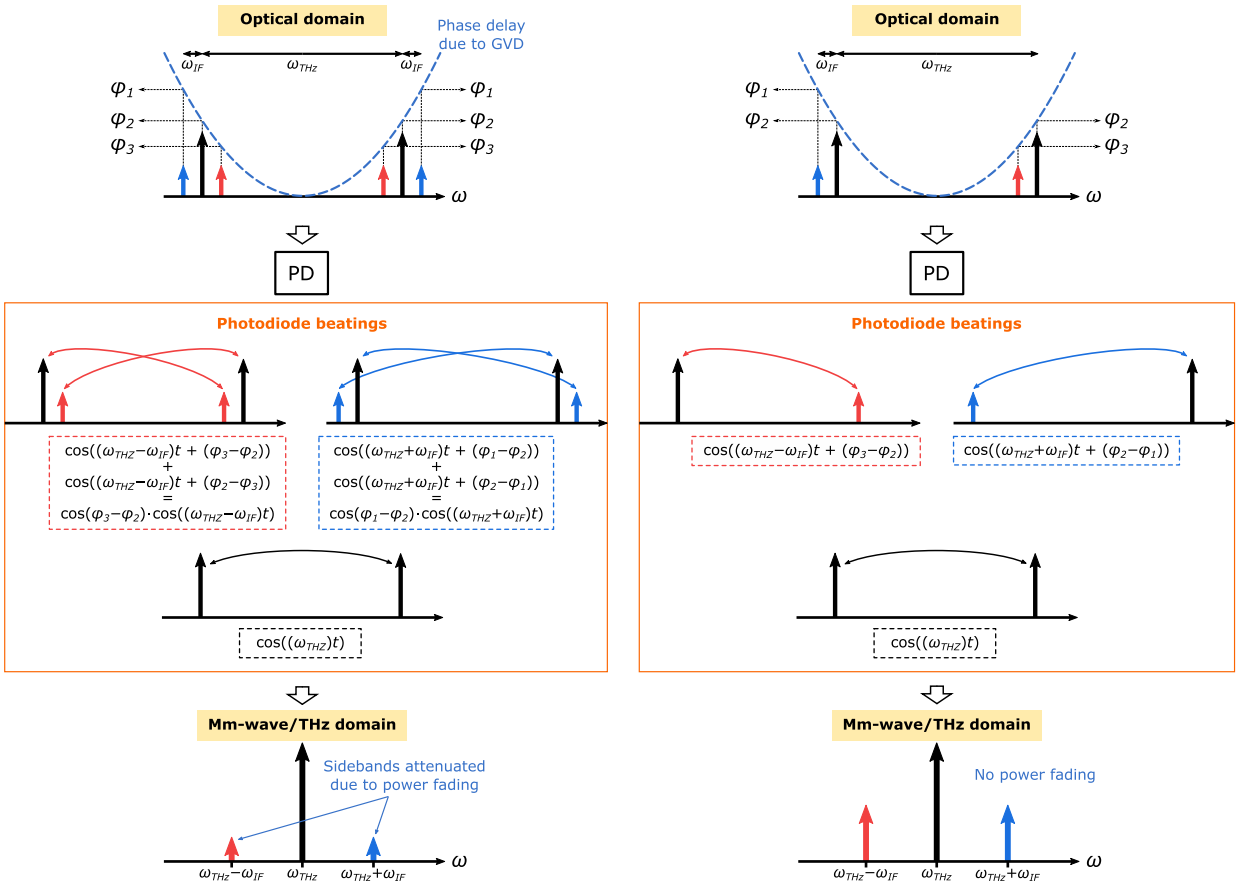

Fig. 2. Phase shifts caused by fiber GVD in dual-λ-mod systems when (a) DSB modulation and (b) SSB modulation are used.

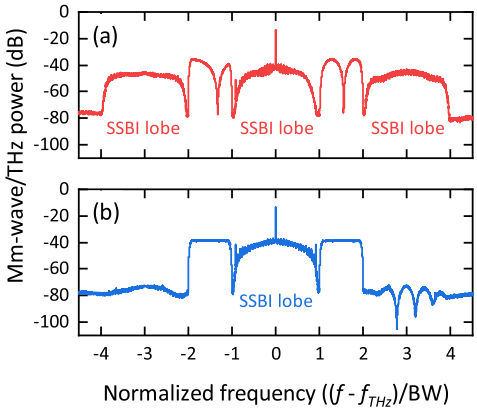

Fig. 3. Spectrum of the mm-wave/THz signal generated when optical (a) DSB-C and (b) SSB-C modulation are used. In both cases the following parameters were used in the simulations: $f_{THz} = 90$ GHz, $f_{IF} = 1.5 \times$ BW, BW $=$ 11 GHz, and $l = 10$ km, where $f_{THz} = (2\pi)^{-1}\omega_{THz}$, $f_{IF} = (2\pi)^{-1}\omega_{IF}$, and BW is the passband bandwidth of the electrical data signal (which in the simulations was a 10-GBd 16-quadrature amplitude modulation signal with a Nyquist roll-off factor of 0.1).

likely to occur if DSB modulation is employed. Since optical SSB formats prevent the appearance of power fading (as can be seen in Fig. 3(b)), they may be more relevant for implementation in dual-λ-mod systems.

B. SSBI

When the optical signal from a dual-λ-mod system is detected by a PD, apart from the carrier-sideband and carrier-carrier beatings depicted in Fig. 2, the optical sidebands also beat with each other. The resultant products from these beatings are typically referred to as SSBI.

When optical SSB-C modulation is used, only one such a signal-signal beating occurs. Its associated SSBI spectrum appears centered around the mm-wave/THz carrier and between the two data sidebands as shown in Fig. 3(b). In the case of DSB-C modulation, there are four signal-signal beatings, and their SSBI spectrum appears around the two data sidebands as shown in Fig. 3(a). The center SSBI lobe is the result of two signal-signal beatings, whereas the two SSBI lobes at the sides are formed by just one beating product each. In any case, the bandwidth of an SSBI lobe is always equal to $2 \times$ BW, where BW is the bandwidth of the optical sideband.

SSBI distorts the mm-wave/THz waveform and can prevent the successful recovery of the information if appropriate techniques to mitigate it are not adopted. One of the most popular such a techniques is allowing a guard band (GB) between the optical sideband and the optical carrier. When the GB bandwidth is equal to the BW, the SSBI products and the resultant mm-wave/THz data sideband do not overlap and the SSBI can

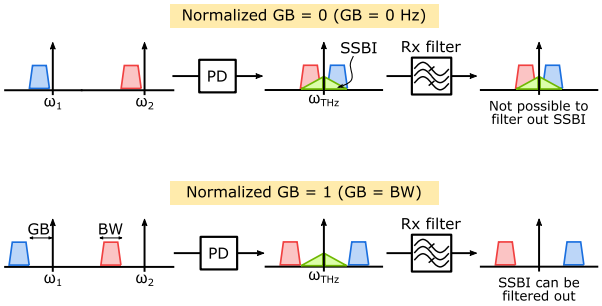

Fig. 4. Impact of GB bandwidth on SSBI mitigation in dual-λ-mod systems. Normalized GB is defined as the bandwidth of the GB divided by BW.

be filtered out completely at the receiver as shown in Fig. 4. The increased system sensitivity obtained by allowing a GB between the optical carrier and sideband, however, comes at the expense of reduced mm-wave/THz bandwidth efficiency. If a GB equal to BW is employed to fully mitigate the SSBI, then, the dual-λ-mod system is four times less spectrally efficient than the conventional heterodyne system depicted in Fig. 1(b). In situations where the mm-wave/THz bandwidth is limited, the bandwidth efficiency of a dual-λ-mod system can be doubled by no using a GB. Although doing this leads to lower system sensitivity due to the presence of SSBI, there are digital SSBI-mitigation algorithms that can be used to improve the performance of a system under this circumstance. As explained in [6], one of the most promising algorithms for dual-λ-mod systems is the transmitter-based pre-distortion. The advantage of this technique over receiver-based algorithms [11] is that it mitigates the SSBI before the interference arises, and therefore it minimizes the amount of unwanted signal that gets transmitted over the wireless channel (as a side comment: in order for this algorithm to work in dual-λ-mod systems, a chromatic dispersion pre-equalization filter needs to be implemented at the transmitter after the SSBI-compensation algorithm).

A key aspect for maximizing a dual-λ-mod system sensitivity – sensitivity here defined in terms of the average optical power required in the PD to produce a certain bit error ratio (BER) – is the carrier-to-signal power ratio (CSPR). CSPR is defined as the power ratio between an optical carrier and its respective data sidebands (i.e., two in the case of DSB modulation or just one for SSB modulation). CSPR is typically controlled by adjusting the optical modulator settings. Since both optical tones go through the same optical modulator in a dual-λ-mod system, the two resultant optical signals have exactly the same CSPR. This is why, in this article, CSPR is referred to in the singular form. As there is always an optimum value of CSPR, which depends on the amount of SSBI-sideband overlap and the noise level in the recovered signal [12], adjusting it is vital to achieve the best system performance.

III. Receiver Configurations and Previous Demonstrations

In this section, the possible wireless receiver configurations for mm-wave/THz single-path systems are discussed and then system demonstrations reported in the literature are reviewed.

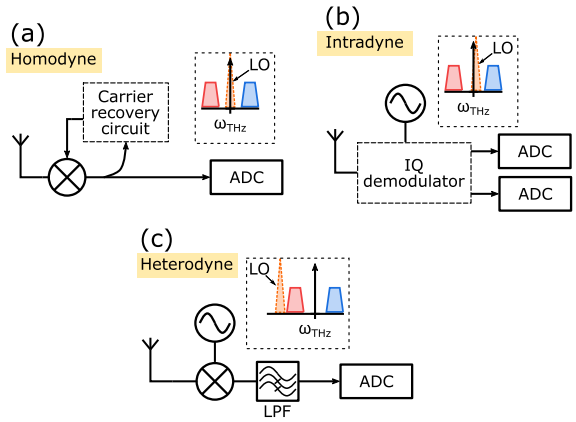

Fig. 5. Wireless DSB receivers: (a) homodyne, (b) intradyne, and (c) heterodyne.

TABLE I
Dual-λ-Mod Systems Reported in the Literature

Freq. (GHz)	Rate (Gb/s)	Format	SMF length	Rx	Ref.
25	0.054	DSB-C	20 km	-	[13]
25.5	1.4	DSB-C	10 km	hom.	[14]
40	2.5	DSB-C	55 km	hom.	[15]
90	0.054	DSB-C	20 km	hom.	[10]

The mm-wave/THz signal generated by a dual-λ-mod system is always a DSB-C signal regardless of the optical modulation (i.e., both optical DSB-C and optical SSB-C modulation will produce a DSB-C signal after photodetection). Hence, the typical DSB receivers employed in wireless communications – homodyne, intradyne, and heterodyne – can be used for down-conversion. The configuration of each of these receivers is shown in Fig. 5. Both homodyne and intradyne can achieve better sensitivity compared to heterodyne downconversion. However, homodyne reception requires a carrier recovery circuit and it is subjected to power fading (even if optical SSB-C formats are used [6]). The intradyne receiver, on the other hand, does not exhibit power fading but requires an IQ demodulator operating at the mm-wave/THz frequency and two analog-to-digital converters (ADCs). Heterodyne down-conversion, although less sensitive, is much simpler to implement and is robust against power fading.

Table I shows some of the mm-wave dual-λ-mod systems reported in the literature to date. Although optical DSB-C modulation is used in the four experiments shown in Table I, no power fading effects are reported in any of them. In [13] and [14] this is believed to be due to the low values of ω_{THz}, ω_{IF} and l (i.e., the mm-wave/THz frequency, the modulating frequency, and the SMF length) used in the experiments, which make the effects of power fading to be very mild. This can be seen in Fig. 6, where the estimated sideband attenuation due to power fading (according to the analysis presented in Section II-A) is plotted for different values of f_{IF} (where $f_{IF} = (2\pi)^{-1}\omega_{IF}$). As can be seen, in Fig. 6(a) and (b) (which correspond to the

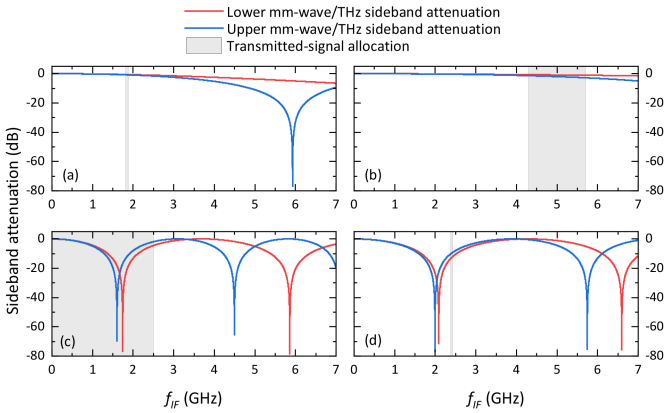

Fig. 6. Estimated mm-wave/THz sideband attenuation due to power fading for the conditions reported in the four experiments shown in Table I: (a) $\omega_{THz} = 25$ GHz and $l = 20$ km; (b) $\omega_{THz} = 25.5$ GHz and $l = 10$ km; (c) $\omega_{THz} = 40$ GHz and $l = 55$ km; and (d) $\omega_{THz} = 90$ GHz and $l = 20$ km. Sideband attenuation values are estimated based on the analysis presented in Section II-A. The grey-filled rectangles represent the allocation of the transmitted signal. $f_{IF} = (2\pi)^{-1}\omega_{IF}$.

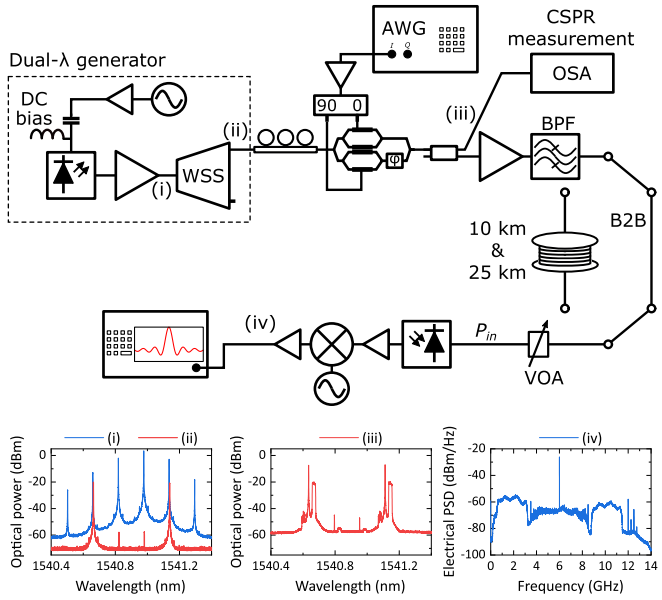

Fig. 7. Experimental arrangement for 60-GHz transmission with a dual-λ-mod system and SSB bias-offset modulation. The insets show the spectrum of: (i) GS laser output, (ii) wavelength selective switch (WSS) output, (iii) IQ modulator output, and (iv) down-converted signal.

transmission conditions reported in references [13] and [14]), the attenuation is quite low. On the other hand, in Fig. 6(c) and (d) (which correspond to the conditions reported in references [15] and [10]) the effect of power fading is much more notorious. Indeed, these two references describe severe signal degradation under such conditions, but they attribute it (the analysis of the system in [15] is performed in [8]) to the first-order term in the Taylor series expansion of the propagation constant (i.e., the one defined by the group velocity) and not to the second order term (i.e., the one defined by the GVD). This is because these references only consider the optical carriers – and not the data sidebands – in their analysis. This, however, yields erroneous results when the values of $\omega_{THz}, \omega_{IF}$, and l are high as explained in Section II-A.

Whereas homodyne downconversion is used in most experiments shown in Table I, no carrier recovery circuit is implemented in any of them. References [10] and [14] reuse the transmitter LO for downconversion, and [15] uses a free-running LO. In a practical system, a mm-wave/THz carrier recovery circuit would be required as outlined in [10]. This, however, may be challenging to implement, especially at THz frequencies. As an alternative to the receiver schemes shown in Fig. 5, envelope or self-homodyne detection can be employed to avoid the use of a receiver LO [16]. However, this reduces system sensitivity [17]. It is not clear what type of receiver configuration is used in [13], but the fact that there is no mention to LO reuse or recovery circuit suggests a heterodyne approach.

IV. Experimental Demonstration At 60 GHz With a Gain-Switched Laser

In this section, experimental results of a dual-λ-mod system operating at 60 GHz are presented. To avoid power fading effects, optical SSB-C modulation is employed. The system is characterized in terms of the BER against the average optical power injected in the PD (P_{in}). Results are measured for optical back-to-back (B2B) transmission and for SMF lengths of 10 km and 25 km. Heterodyne reception is used to minimize receiver complexity. An experimental comparison with a conventional heterodyne photonic system (i.e., the one shown in Fig. 1(a)) is also carried out.

A. Experimental Arrangement

The dual-λ-mod system arrangement is shown in Fig. 7. The dual-λ generator comprised a gain-switched (GS) laser and a wavelength selective switch (WSS). The former, which was based on the direct modulation of an off-the-shelve distributed feedback (DFB) laser, was driven by a CW signal with a frequency of 20 GHz. Hence, the GS-laser output – shown in Fig. 7(a) inset (i) – consisted on multiple optical tones separated by 20 GHz. The optical linewidth of the GS laser tones was around 30 MHz. The WSS was used to select two optical lines from the GS-laser output with a frequency separation of 60 GHz. The two selected lines were then directed to a single WSS output port. The WSS output spectrum is shown in Fig. 7 inset (ii), where it can be seen that the unwanted tones were suppressed by about 40 dB relative to the two carriers used for transmission.

The two selected lines were passed through an IQ Mach-Zehnder modulator (MZM) for optical modulation. In the experiment, the CSPR was set by adjusting the bias levels of the two inner MZMs in the IQ modulator and was measured with a high-resolution optical spectrum analyzer (OSA) after the IQ-MZM as shown in Fig. 7. The SSB-C signal was generated by passing the output signal from the arbitrary waveform generator (AWG) through a 90° hybrid, whose outputs were used to drive the I and Q inputs of the IQ modulator. To ensure maximum sideband suppression in the generated SSB-C signal, the bias level of the outer MZM in the IQ modulator was set at quadrature.

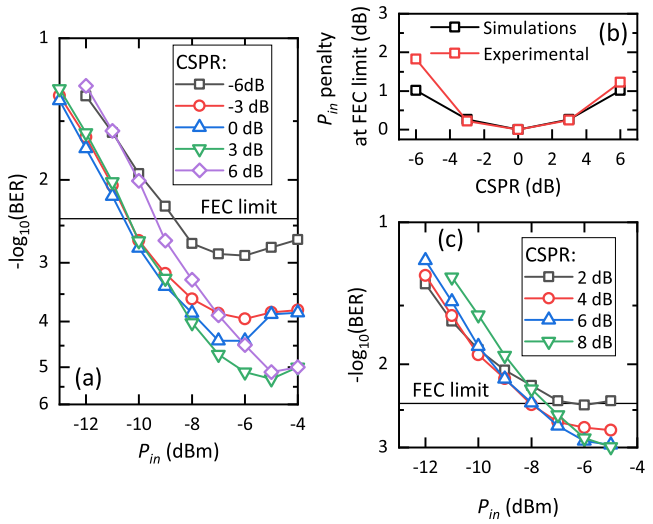

Fig. 8. Results for optical B2B transmission: (a) BER vs. P_{in} curves for a normalized GB of 1 and different CSPRs, (b) experimental and simulation-obtained P_{in} penalty at the FEC limit for different CSPR values, and (c) BER vs. P_{in} curves for a normalized GB of 0.64.

The IQ modulator output for a CSPR of 0 dB is shown in Fig. 7 inset (iii).

A commercial PD was used for generation of the 60-GHz signal, which was subsequently amplified and then down-converted to an IF by using a heterodyne-based receiver formed by an LO and a Schottky diode-based mixer. After digitization of the received signal in an oscilloscope, a standard coherent digital signal processing (DSP) routine – consisting of down-conversion, matched filtering, equalization, and phase noise compensation – was employed for demodulation and BER measurement.

The transmitted signal was a 16-quadrature amplitude modulation (16-QAM) root-raised-cosine (RRC) signal with a symbol rate of 2.5 GBd. As can be seen in Fig. 7 inset (iv), which presents the 60 GHz signal downconverted to an IF of 6 GHz after beating with a 54 GHz LO, the total bandwidth of the 60-GHz signal was 11 GHz. Since a heterodyne receiver was used in the experiments, only the high-frequency sideband from the transmitted 60-GHz signal was digitally demodulated. This sideband was used due to its slightly better BER performance than its low-frequency counterpart. The worse performance at low frequencies is attributed to the higher noise figure of the receiver amplifier near DC.

B. Results for B2B Transmission

Fig. 8 shows the results for B2B transmission. Two different normalized GBs (normalize GB is defined as the bandwidth of the GB divided by BW) were tested in this case: 1 and 0.64. The latter was the minimum allowed by the bandwidth of the RF 90°-hybrid used to generate the SSB signal. Fig. 8(a) shows the BER results for a normalized GB of 1 and different CSPRs. At a P_{in} above -8 dBm, the PD saturates and makes the system nonlinear. In the linear PD regime, optimum performance is obtained for a CSPR of 0 dB, and then the performance degrades for higher and lower CSPRs. Fig. 8(b) plots the P_{in} penalty at the FEC limit for different CSPRs obtained experimentally and also in simulations. As can be seen, there is a good match between them. In the simulations, thermal receiver noise was assumed to dominate over other noise sources such as those discussed in [18] or PD shot noise. This is typically the case in high-frequency wireless systems, where transmitter noise is strongly attenuated by the free-space and mixer down-conversion losses. In spite of not having wireless transmission (and, hence, not being subjected to free-space losses), it seems, according to Fig. 8(b), that the experimental arrangement depicted in Fig. 7(b) was accurately modeled by the simulations.

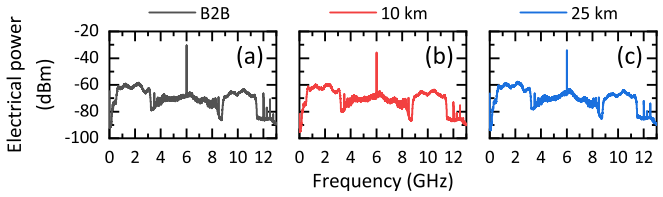

Fig. 9. Spectrum of the down-converted electrical signal for: (a) B2B, (b) 10-km, and (c) 25-km SMF transmission.

Fig. 8(c) shows the BER results for a normalized GB of 0.64. In this case, the intersection of the BER curves with the FEC limit is very close to the PD saturation regime making the quantitative comparison with simulations (where a linear link was assumed) more difficult. In any case, from a qualitative point of view, the results shown in Fig. 8 agree with heterodyne theory, which states that low CSPRs perform better at low P_{in} but worse at high values of P_{in} [12].

C. Results for 10-Km and 25-Km Transmission

All results shown in this section were obtained for an SSB-C signal with a normalized GB of one and a CSPR of 0 dB. Fig. 9 shows the down-converted electrical spectrum (i.e., taken at point iv in Fig. 7) of the transmitted signal for three different SMF transmission lengths: B2B, 10 km, and 25 km. As can be seen, no power dips are present, confirming the robustness of SSB formats against power fading in dual-λ-mod systems. Fig. 10(a) shows the BER curves for each transmission distance. It can be seen that almost identical performance is obtained for the B2B and 10-km cases. On the other hand, a ∼2 dB penalty is observed for the 25-km transmission. This penalty arises due to the decorrelation suffered by the two optical tones from the dual-λ-mod source upon fiber propagation, which progressively increases the phase noise of the generated 60-GHz signal. This can be seen in Fig. 10(b), where the phase noise of the received 60-GHz signal (when no data was modulated into the system) is shown for each SMF transmission length. As can be seen, for frequencies higher than 100 MHz, the phase noise for 25 km is around 5 dB higher than that for B2B and 10 km. The constellation diagram for 25 km in Fig. 10(a) shows how this increase in phase noise distorts the received symbols (especially those in the outer constellation rings), increasing the BER.

As decorrelation is higher for sources with wider optical linewidths, a lower penalty could be obtained for 25 km by injection locking the GS source to a low-linewidth master laser

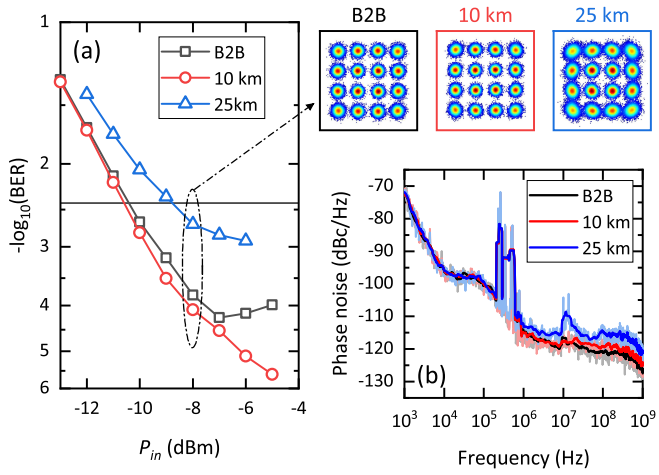

Fig. 10. (a) BER vs. P_{in} curves for B2B, 10 km, and 25 km of SMF transmission and the associated constellation diagrams for a P_{in} of −8 dBm; and (b) phase noise in the received signal for each different SMF transmission length.

as in [19]. This would reduce the linewidth of the optical tones from 30 MHz to less than 1 MHz ensuring a longer coherence length and excellent correlation between them even after 25-km transmission. Nevertheless, Fig. 10(a) shows how, even for a transmission length of 10 km, a simple dual-λ-mod source generated using the direct modulation of a cost-effective DFB laser yields good system sensitivity.

D. Comparison Between dual-λ-Mod and Conventional Heterodyne Systems

Fig. 11(a) and (b) show the optical transmitter configurations for the dual-λ-mod and conventional heterodyne systems, respectively. As can be seen, compared to the former, the conventional heterodyne system requires the addition of the following components: two narrow-band filters, a tunable optical delay line, two 3-dB couplers, and a polarization controller. This increases considerably the overall system complexity and also its associated loss. Another difference is that, in the conventional heterodyne system, the bias levels of the two inner MZMs in the IQ modulator need to be set at the minimum transmission point in order to suppress the optical carrier. This supression can be seen in the inset of Fig. 11(b), which shows the optical spectrum at the output of the conventional heterodyne transmitter.

Fig. 12(c) shows the BER curves of the two systems for the three different SMF transmission lengths: B2B, 10 km, and 25 km (the dual-λ-mod BER curves are those shown in Fig. 10(a)). Regarding the conventional heterodyne system, BER curves for all SMF lengths exhibit the same performance. This is because such a system allows for the compensation of the decorrelation between optical tones arising from SMF transmission through the tunable optical delay line (albeit at the expense of additional complexity and the requirement for optimum delay calculation) [20]. A P_{in} penalty of around 2.8 dB at the FEC limit was obtained between the two systems for B2B transmission. This agrees quite well with simulation results, which predict a 3-dB penalty between them as shown in Fig. 12(b). The main objective of the simulations was to confirm the relative penalty between the two systems, rather than replicate absolute system performances. This is why the x axis in Fig. 12(b) is given in a variable proportional to P_{in} (in dB) and not in optical power (absolute optical power values depend on various factors – such as PD responsivity, receiver losses, amplifier gains, etc. – which were not included in the simulations).

Following the analysis presented in the supplementary information of [6], for both the SSB-C dual-λ-mod and conventional heterodyne systems, it is relatively straightforward to prove the following statement: when the CSPR is set to 0 in an SSB-C dual-λ-mod system, the amplitude of each generated mm-wave/THz sideband is half the amplitude of the data signal generated by the conventional transmitter (assuming a fixed value of P_{in} in both systems). This means that each sideband of the mm-wave/THz signal generated with a dual-λ-mod system has four times less power than the mm-wave/THz data signal generated with the conventional transmitter (since power is proportional to the square of the amplitude). Since received electrical power is proportional to mm-wave/THz power, if a heterodyne receiver is employed in both systems (i.e., only one sideband is used for demodulation in the dual-λ-mod system), the electrical signal-to-noise ratio (SNR) in the dual-λ-mod system will be four times less than that in the conventional system (assuming both systems are receiver-noise limited so that electrical SNR is determined by downconverted sideband power and receiver noise). Hence, the mm-wave/THz power in the dual-λ-mod system would need to be increased by four in order to match the electrical SNR of the conventional system. Since mm-wave/THz power is proportional to the square of the optical power detected by the PD, increasing by four the mm-wave/THz power corresponds to doubling the optical power, which is why there is a 3-dB P_{in} penalty between the two systems.

On the other hand, if a homodyne receiver as the one depicted in Fig. 5(a) is used in both the conventional and dual-λ-mod systems, then both systems should exhibit the same performance for B2B optical transmission. This is because this receiver would yield the same performance for the conventional system but would increase the electrical SNR achieved with the dual-λ-mod system by four (since both sidebands would be coherently added, doubling the amplitude of the downconverted sideband). However, this receiver would make the dual-λ-mod system susceptible to power fading, rendering it impractical for long optical transmission distances. If an intradyne receiver is used, there should be a 1.5-dB P_{in} penalty between the two schemes since receiver noise bandwidth and, hence, receiver noise power – rather than amplitude – would be half for the conventional transmitter. In this case, however, the dual-λ-mod would not suffer from power fading.

Dual-λ-mod systems, hence, can yield similar performance as conventional heterodyne transmitters while greatly reducing the system complexity. As outlined at the beginning of this section, the conventional transmitter required the addition of two narrow-band filters, a tunable optical delay line, two 3-dB couplers, and a polarization controller. The cost of all these components amounts to several thousands of euros, however it is complicated to estimate the cost difference between the two systems if both

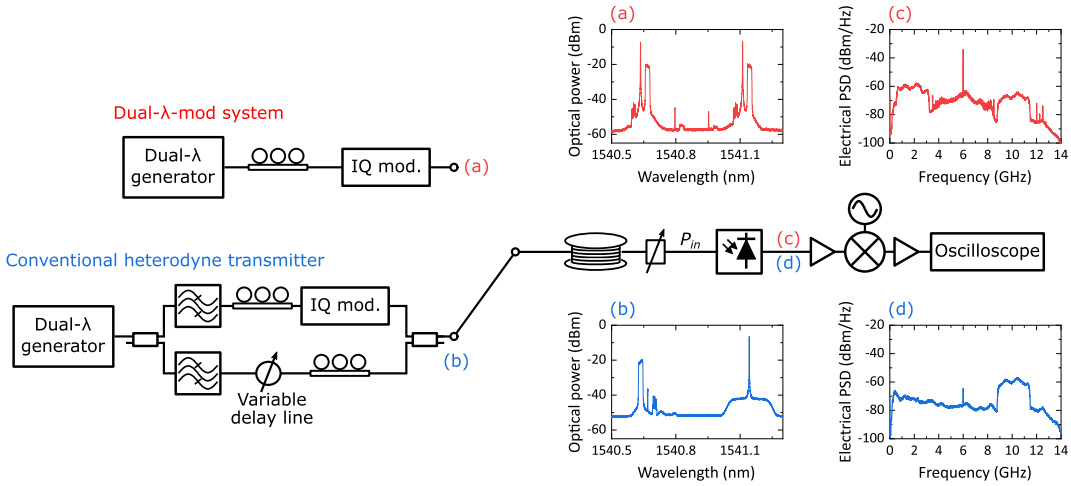

Fig. 11. Experimental arrangement, optical spectrum generated by (a) the dual-λ-mod and (b) conventional heterodyne system, and electrical spectrum of the downconverted signal after 25 km of SMF for (a) the dual-λ-mod and (b) conventional heterodyne system.

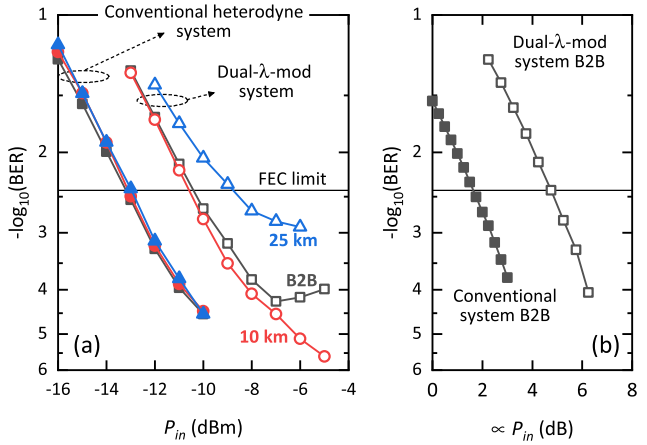

Fig. 12. BER vs. P_{in} curves for both systems (a) experimental results for different SMF transmission lengths and (b) simulation results for optical B2B transmission.

are integrated in a photonic chip, as such a cost difference would depend heavily on volume. In spite of this, it is clear that the lower chip area required by the dual-λ-mod system can led to massive cost savings if both are to be produced on industrial scales.

V. Conclusion

The implementation of cost-efficient optical systems for the generation of mm-wave and THz signals is of paramount importance for the dense deployment of wireless systems. Due to their simplicity, dual-λ-mod photonic mm-wave/THz transmitters are an attractive alternative to conventional heterodyne systems. In this article, dual-λ-mod systems are analysed both through simulations and experimentally. The main impairments affecting these systems – optical dispersion and SSBI – are discussed. It is concluded that dual-λ-mod systems employing optical DSB formats do suffer from power fading. Optical SSB formats, on the other hand, prevent the appearance of power fading and are a good candidate for high-speed dual-λ-mod systems. Using a GS laser, a 60-GHz SSB dual-λ-mod system transmitting 2.5-GBd 16-QAM signals is demonstrated. A P_{in} penalty of just 2.8 dB is measured with respect to the conventional heterodyne transmitter at a BER of 10^{-3} for optical B2B and 10 km transmission. It is also discussed how the employment of an intradyne receiver can decrease the P_{in} penalty between the two systems down to 1.5 dB. This article, hence, presents a significantly simpler mm-wave/THz photonic system that only exhibits a moderate penalty with respect to conventional systems. The reduced complexity associated to the demonstrated system aids photonic integration and the deployment of cost-effective mm-wave/THz transport and generation networks.

References

[1] T. Nagatsuma, G. Ducournau, and C. C. Renaud, "Advances in terahertz communications accelerated by photonics," *Nature Photon.*, vol. 10, no. 6, pp. 371–379, 2016, doi: 10.1038/nphoton.2016.65.

[2] K. Mallick et al., "Nonlinearity optimization in FSO transport system and generation of 24-GHz MW signal based on OADM scheme and external modulation technique," *Opt. Quantum Electron.*, vol. 53, no. 9, pp. 1–10, 2021, doi: 10.1007/s11082-021-03170-w.

[3] K. Mallick et al., "Bidirectional OFDM based MMW/THzW over fiber system for next generation communication," *IEEE Photon. J.*, vol. 13, no. 4, Aug. 2021, Art. no. 7301207.

[4] Y. Y. Lin, P. S. Chang, Y. T. Chen, C. Y. Li, and H. H. Lu, "A Fiber-FSO-5 G wireless convergent system for simultaneous transmission of 5 G MMW and 5G NR Sub-THz signals," in *Proc. Conf. Lasers Electro- Opt.*, 2022, vol. 40, pp. 2348–2356.

[5] S. Jia et al., "0.4 THz photonic-wireless link with 106 Gb/s single channel bitrate," *J. Lightw. Technol.*, vol. 36, no. 2, pp. 610–616, Jan. 2018.

[6] L. Gonzalez-Guerrero and G. Carpintero, "Coherent photonic terahertz transmitters compatible with direct comb modulation," *Sci. Rep.*, vol. 12, no. 1, pp. 1–10, 2022, doi: 10.1038/s41598-022-13618-y.

[7] T. Nagatsuma et al., "Real-time 100-Gbit/s QPSK transmission using," in *Proc. Int. Topical Meeting Microw. Photon.*, 2016, vol. 1, pp. 27–30.

[8] J. Ma, J. Yu, C. Yu, X. Xin, J. Zeng, and L. Chen, "Fiber dispersion influence on transmission of the optical millimeter-waves generated using LN-MZM intensity modulation," *J. Lightw. Technol.*, vol. 25, no. 11, pp. 3244–3256, Nov. 2007.

[9] J. M. Fuster, J. Marti, J. L. Corral, V. Polo, and F. Ramos, "Generalized study of dispersion-induced power penalty mitigation techniques in millimeter-wave fiber-optic links," *J. Lightw. Technol.*, vol. 18, no. 7, pp. 933–940, Jul. 2000.

[10] P. T. Dat, A. Kanno, K. Inagaki, and T. Kawanishi, "High-capacity wireless backhaul network using seamless convergence of radio-over-fiber and 90-GHz millimeter-wave," *J. Lightw. Technol.*, vol. 32, no. 20, pp. 3910–3923, Oct. 2014.

[11] Z. Li et al., "Comparison of digital signal-signal beat interference compensation techniques in direct-detection subcarrier modulation systems," *Opt. Exp.*, vol. 24, no. 25, pp. 29176–29189, 2016.

[12] L. Gonzalez-Guerrero et al., "Comparison of optical single sideband techniques for THz-Over-Fiber systems," *IEEE Trans. THz Sci. Technol.*, vol. 9, no. 1, pp. 98–105, Jan. 2019.

[13] J. James, P. Shen, A. Nkansah, X. Liang, and N. J. Gomes, "Nonlinearity and noise effects in multi-level signal millimeter-wave over fiber transmission using single and dual wavelength modulation," *IEEE Trans. Microw. Theory Techn.*, vol. 58, no. 11, pp. 3189–3198, Nov. 2010.

[14] S. Rommel et al., "Real-time high-bandwidth mm-wave 5G NR signal transmission with analog radio-over-fiber fronthaul over multi-core fiber," *Eurasip J. Wireless Commun. Netw.*, vol. 2021, no. 1, 2021, Art. no. 43, doi: 10.1186/s13638-021-01914-6.

[15] J. Yu, Z. Jia, L. Yi, Y. Su, G. K. Chang, and T. Wang, "Optical millimeter-wave generation or up-conversion using external modulators," *IEEE Photon. Technol. Lett.*, vol. 18, no. 1, pp. 265–267, Jan. 2006.

[16] P. T. Dat, A. Kanno, N. Yamamoto, and T. Kawanishi, "Seamless convergence of fiber and wireless systems for 5G and beyond networks," *J. Lightw. Technol.*, vol. 37, no. 2, pp. 592–605, Jan. 2019.

[17] G. Carpintero, S. Hisatake, D. D. Felipe, R. Guzman, T. Nagatsuma, and N. Keil, "Wireless data transmission at terahertz carrier waves generated from a hybrid InP-Polymer dual tunable DBR laser photonic integrated circuit," *Sci. Rep.*, vol. 8, no. 1, pp. 1–7, 2018, doi: 10.1038/s41598-018-21391-0.

[18] A. J. Lowery, "Amplified-spontaneous noise limit of optical OFDM lightwave systems," *Opt. Exp.*, vol. 16, no. 2, pp. 860–865, 2008.

[19] C. Browning et al., "Gain-switched optical frequency combs for future mobile radio-over-fiber millimeter-wave systems," *J. Lightw. Technol.*, vol. 36, no. 19, pp. 4602–4610, Oct. 2018.

[20] T. Shao et al., "Chromatic dispersion-induced optical phase decorrelation in a 60 GHz OFDM-RoF system," *IEEE Photon. Technol. Lett.*, vol. 26, no. 20, pp. 2016–2019, Oct. 2014.